An Ultra High Frequency Radio Frequency Identification Compatible Circular Polarized Microstrip Antenna Array

Md Yousuf Hossain[1], Narayan Chandra Nath[2], OMAR FARUQ[3], Changzhou Hua[4]

[1]*Faculty of Electrical Engineering and computer science, Information and Communication system, Ningbo University, Ningbo-315000, China.*

[2]*Department of Physics/ Electrical Engineering, Control, Microsystems, Microelectronics, University of Bremen, Bremen-330440-28334, Germany.*

[3]*Department of Electrical and Electronic Engineering, Bangladesh University of Engineering and Technology, Dhaka-1000, Bangladesh.*

[4]*Faculty of Electrical Engineering and Computer Science, Ningbo University, Ningbo-315000, China.*

Abstract

This study focuses on the development, simulation, and practical validation of a metal-only microstrip patch antenna and its array designed to increase gain. The antenna is specifically designed to meet the growing demand for reliable and efficient RFID systems in various fields, such as asset tracking, inventory management, and smart logistics. Our design utilizes a truncated patch with an air substrate to achieve high gain and circular polarization. The antenna's dimensions measure 468 × 188 × 31 mm³ and deliver impressive performance metrics, boasting a return loss |S11| of -18.21 dB and an estimated gain exceeding 10.6 dBi. These figures compare favorably with the simulated results, which indicate an |S11| of -20.8 dB and a total gain of 11.2 dBi. Our microstrip antenna array demonstrated consistent Circular Polarization quality throughout the radiation angle, with an Axial Ratio of less than 3 dB. This antenna has emerged as a compelling solution for UHF-band RFID technology to meet the demands of various real-world applications.

Keywords: *Microstrip Antenna Array, RFID Technology, UHF, Antenna Design, Antenna Polarization.*

1. Introduction

In the realm of wireless communication and identification technologies, Radio-Frequency Identification (RFID) stands as a cornerstone for seamless and pervasive connectivity [1]. Operating within the Ultra High Frequency (UHF) band, RFID systems have become integral to applications ranging from inventory management and supply chain logistics to access control and asset tracking [2]. The efficiency of these systems heavily relies on the performance of the RFID antennas [3], especially in scenarios where factors such as orientation variability, interference, and communication range come into play [4]. Antennas of various specified forms, including square, circular, and octagonal, were suggested over time [5]. A truncated-shaped antenna consisting of a single element was proposed in [6]. The antenna is 254×254×18 mm3 in total dimension. To design it, an air-substrate patch antenna is employed. The antenna has a gain of 9 dBi and an Axial Ratio (AR) of less than 3 dB. In [7], a 1×2 array RFID antenna operating in the 2.4 GHz ISM band was suggested. The dimension of the suggested antenna is 120× 73×1.5 mm3 overall. The suggested antenna's S11 is around -16.10 dB, and it achieves a gain of roughly 7.50 dBi. This paper is dedicated to the design, development, and evaluation of a specialized RFID-compatible antenna optimized for operation within the UHF band. In this case, Circular Polarization (CP) was chosen because of its intrinsic

Corresponding author: *OMAR FARUQ (smomarfaruq99@gmail.com)*
Received: *17 April 2024*; Revised: *9 May 2024*; Accepted: *12 May 2024*; Published: *20 May 2024*

benefits, which include robustness against multipath propagation and signal fading, as well as orientation insensitivity. The integration of a 1×2 array configuration further enhances the antenna's capabilities, promising higher gain and improved coverage. The design of a 1×2 array of circularly polarized microstrip antennas is shown in this paper. An air-substrate truncated patch antenna is used to create the circular polarization. Researchers have developed various antenna designs, including circularly polarized antennas and their arrays. One such design is the broadband series-fed circularly polarized microstrip antenna array, which consists of four rotating microstrip antennas linked to a central circularly polarized patch antenna. This antenna exhibits an impressive impedance bandwidth spanning from 3.77 to 6.30 GHz, with an AR of 43.2% and a maximum gain of 12.1 dBi [8]. Another innovative design is the triangular microstrip antenna array, designed for applications in the L-band spectrum, including military usage, global positioning systems, and digital audio broadcasting. The array has a return loss of less than -20 dB and an impressive gain of approximately 12 dB. The individual patch within the array contributes to a gain of 6.31 dB. The Elliptical MicroStrip Patch Antenna (EMSPA) is designed to operate within the ISM band range of 2.4 GHz to 2.5 GHz, using coaxial probes for feeding [9]. The study aims to determine enhanced gain and reduced |S11| levels across different frequencies in the Industrial, Scientific, and Medical (ISM) band. The EMSPA is designed and simulated using various software tools, including MATLAB, to estimate performance characteristics such as s-parameters, voltage standing wave ratio, EH fields, radiation pattern, current distribution, gain, elevation, and azimuthal radiation patterns [10]. A UHF-RFID circularly polarized reader antenna is presented, with an impedance bandwidth of 880-960 MHz and a voltage standing wave ratio less than 1.5 [11]. A microstrip patch antenna designed for 865 MHz within the UHF band is also presented. The study found a correlation between antenna length and operational frequency, with increased antenna length reducing operating frequency and increasing |S11|, suggesting improved reflection coefficients and minimized power losses [12]. The frequency decrease and corresponding increase in |S11| were observed with an escalation in antenna width, suggesting a nuanced relationship between these parameters. An asymmetrical circular slotted microstrip antenna was developed for RFID and CP applications [13]. The study found that increasing slot size corresponded to a drop-in resonance frequency. Additional slits were introduced to enhance tunability and adjust the operational band [14].

Institute of Electrical and Electronic Engineering (IEEE) letter presented an antenna designed for RFID applications, focusing on wideband isolation. The antenna consisted of a radiative patch and a ground plane connected to a branch-line coupler [15]. Following construction, the prototype antenna demonstrated an AR of approximately 2 dB within the frequency range of 860 MHz to 940 MHz and an |S11| value of around -18 dB. Remarkably, the antenna achieved a broad bandwidth of approximately 65 MHz (864–929 MHz), showcasing a notable -25 dB isolating characteristic between the Tx and Rx ports. This design successfully aligns with the RFID bands in Europe (865–869 MHz) and the United States (902–928 MHz), affirming its suitability for diverse frequency regulations. In the exploration documented in [16], a project study introduced a circularly polarized octagonal-form microstrip patch antenna, powered by coaxial feed. The motivation for designing and analyzing this antenna stemmed from its intended application in RFID reader systems. Various feeding techniques for a 2.4 GHz microstrip patch antenna have been put forth. The covered design approaches include the Rectangular Microstrip Antenna (RMSA) with microstrip feed, microstrip inset line feed, and microstrip quarter-wave line feed [17]. Notably, the quarter-wave line feed emerged with the most favorable return loss, registering at -19.95 dB.

In this paper, in Introduction (Chapter 1), the research and research background are presented. In chapter 2, the method of the research is presented. In chapter 3, the structural design of antennas is presented. In chapter 4, we present an analysis of the following research and the results of the analysis. And the last section of the paper is the conclusion of the research.

2. Methodology

The methodology employed in this research entails a comprehensive approach combining software simulation, data analysis, precise measurements, and experimental setups. The design and simulation of the antenna are executed using HFSS software (high-frequency structure simulator), while Origin Pro 2018 is utilized for data analysis and graphing of both simulated and measured data. To ensure efficient signal transmission during data measurement, a 50-ohm coaxial feed, meticulously welded, is integrated as the feeder. The evaluation of the antenna's electrical characteristics relies on the precise measurements obtained from an Agilent vector network analyzer, specifically the Agilent E8361C model, emphasizing accuracy in assessment. Additionally, in scenarios where an anechoic chamber is utilized to evaluate antenna pattern and gain, strict adherence to the coordinate axis direction in the simulation model is emphasized, highlighting the importance of consistency between simulation and experimental conditions. The antenna design for a metal-only microstrip patch antenna focuses on improving efficiency and reliability in RFID systems. The antenna's dielectric constant is adjusted to minimize losses and utilize air as the dielectric medium. A 30 mm-high side boundary wall is built to enhance the AR and enable feed line integration. A simple feeding mechanism is developed using a microstrip line with a width of 2 mm. CP is used to rotate an electromagnetic field, ensuring constant signal reception regardless of the antenna's orientation. This approach is aimed at enhancing RFID system operation and addressing the need for improved performance and reliability. The dimension of the dual panel antennas is 468 x 188 x 31 mm³, which includes the patch, ground, and boundary walls. Four Teflon cylinders are carefully placed to ensure structural integrity and exact patch placement. The antenna's center-to-center spacing of 234 mm corresponds to the operational frequency, resulting in synergy and increased radiation efficiency. This comprehensive test methodology ensures a thorough evaluation of the antenna's performance characteristics, offering valuable insights into its real-world functionality. In Figure 16, a direct comparison between the simulated and measured reflection coefficient curves of the single-ported antenna port is presented, offering valuable insights into the agreement between theoretical predictions and practical observations. The last stage of the antenna design process involves the building of a dual array arrangement, which is a strategic move aimed at increasing the antenna's gain.

3. Materials: Structural Design of the Antenna

3.1. Construct a simple square patch

Embarking on the construction journey of a "metal-only microstrip patch antenna and its array," the initial focus lies on a crucial and fundamental step: the creation of a simple square patch. This section serves as a detailed guide, unveiling the step-by-step process to construct this foundational element of the antenna, in Figure 1. The significance of this initial phase cannot be overstated, as the simple square patch lays the groundwork for the entire antenna structure and its subsequent array configuration. By beginning with the construction of this basic element, we pave the way for a comprehensive understanding of the antenna design, its intricacies, and the subsequent steps that will unfold in the pursuit of optimal performance and functionality [18]. The initial step involved creating a simple rectangular shape, and the microstrip patch dimensions were set at L = W = 139 mm. This symmetry ensures a balanced design, which is often desirable in microstrip patch antennas. The thickness of the patch is specified as 1 mm, contributing to the overall geometry of the antenna.

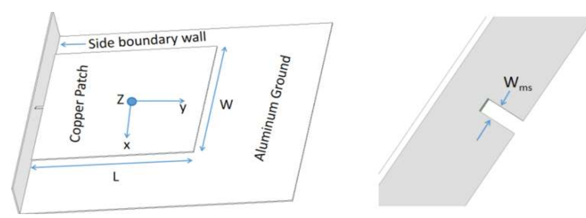

Figure 1. Initial square patch design.

3.2. Substrate Selection and Dimensions

The dielectric constant of the substrate is a critical factor influencing the antenna's electrical characteristics. In this design, air is chosen as the dielectric medium, possessing a dielectric constant of 1. This decision is strategic, as it minimizes dielectric losses within the antenna structure, promoting efficient signal propagation. The substrate height is set at 20 mm, indicating the distance between the microstrip patch and the ground plane (aluminum) [19]. This dimension plays a vital role in determining the antenna's impedance, radiation pattern, and overall performance. A careful balance is struck with this chosen height to achieve optimal resonance at the specified frequency of 920 MHz.

3.3. Side boundary wall and feeding system

The antenna design aims to improve CP characteristics and enhance AR by constructing a 30 mm side boundary wall. The antenna is fed via a 50-ohm microstrip line, with a width of 2 mm, ensuring impedance matching and efficient power transfer. The design incorporates dimensions and features carefully selected to meet specific requirements. The use of air as the dielectric substrate and the specified dimensions and feeding system aim to achieve resonance at the target frequency and enhance circular polarization. As the design progresses, these parameters will be subject to simulation and experimental validation to optimize performance in applications like UHF RFID technology.

3.4. The truncated structure to achieve circular polarization

The pursuit of enhanced performance and reliability in RFID systems has driven antenna designers to explore innovative solutions. One such strategy involves the deliberate introduction of a truncated structure to achieve CP. This section delves into the rationale, design considerations, and implications of incorporating a truncated structure for CP in RFID antenna design. Asymmetric construction emerges as a key design principle, addressing the unique requirements of RFID applications and ultimately enhancing system functionality. CP is characterized by the rotation of the electromagnetic field, allowing for consistent signal reception regardless of the relative orientation between the transmitting and receiving antennas [20].

Unlike linearly polarized antennas, circularly polarized antennas offer improved multipath performance and resilience to changes in orientation—a crucial advantage in dynamic RFID environments. The decision to pursue CP is rooted in the recognition of these advantages and the desire to optimize RFID system functionality. Achieving CP requires breaking away from the traditional symmetrical design commonly associated with linearly polarized antennas. Asymmetric construction is a key prerequisite for circular polarization, and in the context of RFID antennas, this departure from symmetry becomes particularly significant.

The truncated structure, as illustrated in Figure 2, introduces deliberate asymmetries within the antenna design. One effective method to achieve this is by trimming off the opposing edges of the antenna patch.

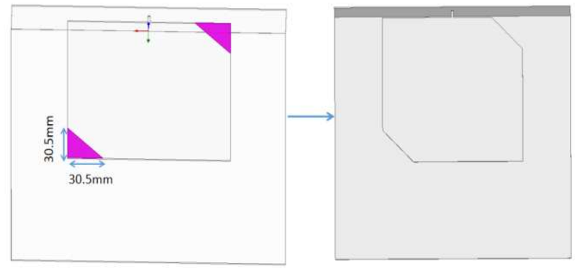

Figure 2. The truncated structure to achieve circular polarization.

The patch's edges are cut by 30.5 mm to ensure circular polarization, a feature that facilitates the generation and reception of circularly polarized waves. These design considerations are crucial to achieving the desired resonance at the RFID system's operational frequency (920 MHz) and ensuring optimal CP characteristics [21]. The advantages of CP extend beyond theoretical considerations, particularly in RFID applications where reliable and efficient data communication is crucial. The intentional asymmetry introduced by the truncated structure addresses challenges posed by varying orientations, reflections, and multipath propagation, resulting in an antenna well-suited to the dynamic RFID environment. To ascertain the effectiveness of the truncated structure in achieving circular polarization, extensive experimental validation is essential. This involves measurement and analysis of key antenna parameters, including return loss |S11|, AR, and radiation patterns [22].

3.5. Finalize antenna array layout

The final stage of antenna design involves the construction of a dual array configuration, which enhances the antenna's gain, a crucial parameter for system performance. This section details the design details, including dimensions, components, and optimized functionality. The dual array configuration, featuring a 1x2 array layout, is a powerful technique for boosting the antenna's gain, a measure of its ability to direct or concentrate radiated energy, in Figure 3. This configuration is ideal for applications requiring enhanced communication capabilities, such as RFID systems, as it offers improved performance and increased signal strength.

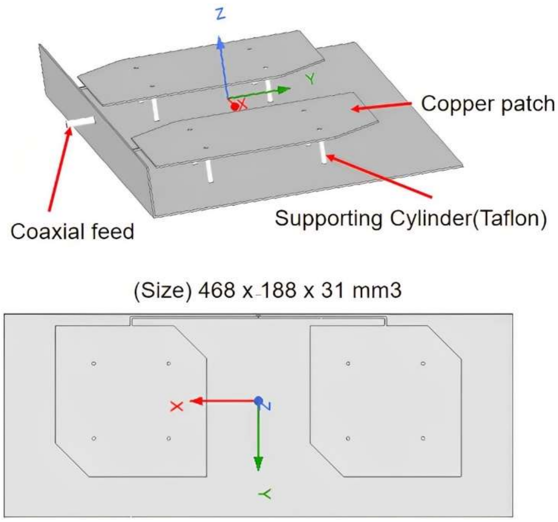

Figure 3. Finalize dual-array antenna layout.

The dual array configuration has a design that spans 468 x 188 x 31 mm³, including the patch, ground, and border wall. Each component maintains a consistent thickness of 1 mm, contributing to the overall antenna geometry. The dimensions are chosen to align with resonance frequency and desired performance characteristics. Four Teflon cylinders, each 22 mm long and 1.5 mm radius, are strategically incorporated to ensure structural integrity and precise patch positioning. This not only maintains the antenna's stability but minimizes potential losses by optimizing the spatial relationship between patches and the ground plane. The dual array configuration positions the two patches at a center-to-center separation of 234 mm. This spacing is strategically chosen to approximate λ/2 (half-wavelength), a key consideration in array design. This separation aligns with the antenna's operational frequency, ensuring that the patches work synergistically to achieve constructive interference and enhance overall radiation efficiency. A 50-ohm coaxial feed line has been employed to mitigate signal losses and ensure efficient power transfer to the antenna [23].

4. Result and Analysis

4.1. Simulation results of the single element design

The single-element design of the "metal-only micro-strip patch antenna and its array" has undergone comprehensive simulation, yielding noteworthy results that underscore its potential for high-performance applications. In this section, we delve into the key findings, including a high gain of 9.1 dB at 920 MHz, an acceptable return loss of approximately -18.94 dB, a promising realized gain of 8.94 dB, and an impressive AR of 1.60 dB. Furthermore, the examination of the radiation pattern, as shown in Figure 4, shows the CP of the antenna, providing significant data about its directional capabilities. The return loss of approximately -18.94 dB signifies the effectiveness of the antenna in minimizing reflected signals back to the source.

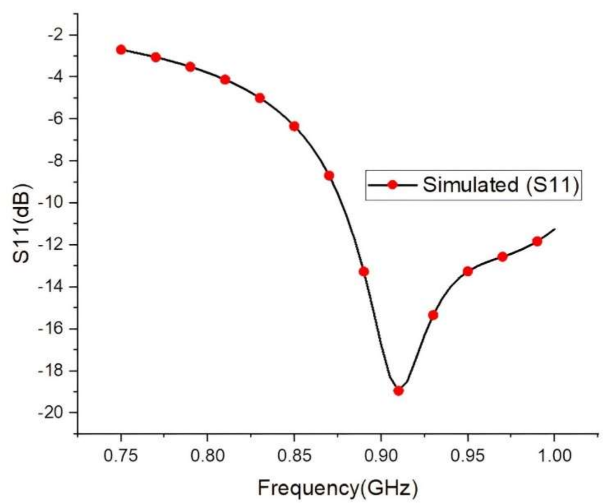

Figure 4. Simulated |S11| for the single element design.

The antenna's performance is enhanced by its excellent impedance matching characteristics, a lower return loss, and an impressive AR of 1.60 dB. CP is crucial in certain applications, and a lower AR is preferred for close-to-ideal circular polarization, in Figure 5. The single-element design excels in circular polarization, demonstrating its suitability for maintaining polarization purity. The antenna's high gain of 9.1 dB at 920 MHz is a critical metric for effective signal amplification. The realized gain, which accounts for system losses, was 8.94 dB, reaffirming the high gain observed in the simulation and highlighting the efficiency of the antenna in practical scenarios, considering real-world losses.

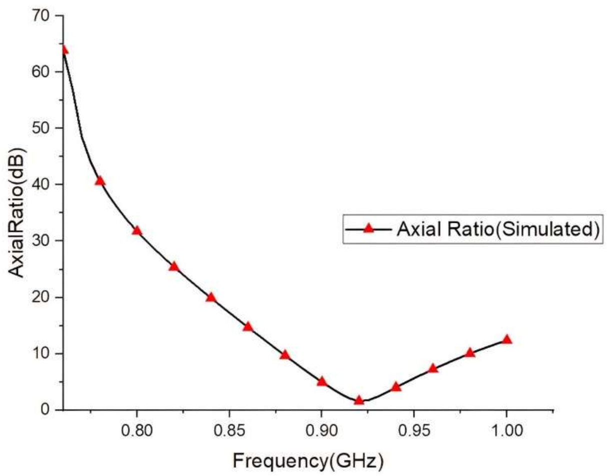

Figure 5. Simulated Axial Ratio for the single element design.

Overall, the antenna's performance is attributed to its excellent impedance matching and CP characteristics, shown in Figure 6.

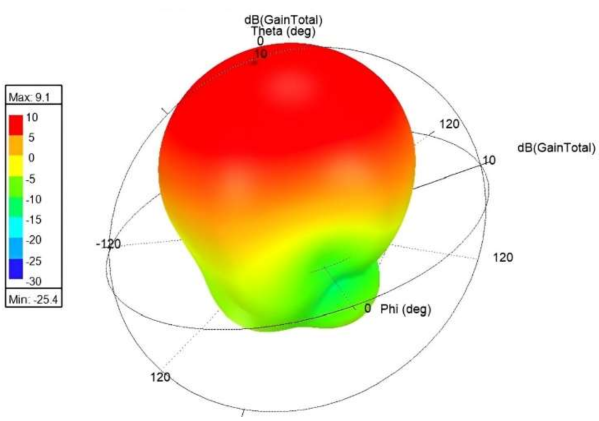

Figure 6. Simulated Gain of the single element design.

The significance of the AR in CP cannot be overstated, as it directly influences the quality of communication systems and satellite links that rely on polarization diversity, shown in Figure 7. The closer the AR gets to 0 dB, the more circular the polarization becomes, indicating a superior performance in mitigating signal distortions caused by changes in polarization during propagation. In the examination of the single-element design, the simulated radiation patterns, as depicted in Figure 8, provide crucial insights into the antenna's polarization characteristics. Observing the radiation pattern at phi = 00 reveals the presence of right-hand circular polarization, a significant attribute for applications requiring robust signal integrity. The 3 dB beam width of the polarization at this azimuthal angle measures approximately 640, indicating a broad coverage area in the horizontal plane. Similarly, at phi = 900, the radiation pattern continues to exhibit right-hand circular polarization, with a slightly wider 3 dB beam width of around 670. These findings underscore the antenna's versatility, showcasing its ability to maintain CP while offering adaptable coverage patterns, making it a promising candidate for diverse communication scenarios and satellite applications [24]. In conclusion, the simulation results of the single-element design showcase a comprehensive set of positive attributes. The combination of a high gain of 9.1 dB, a realized gain of 8.94 dB, an acceptable return loss of approximately -18.94 dB, and an impressive AR of 1.60 dB collectively positions the antenna as a promising candidate for high-performance communication systems. These simulation results lay a solid foundation for further exploration, and the insights gained contribute significantly to the understanding of the antenna's capabilities, paving the way for practical implementations in real-world scenarios.

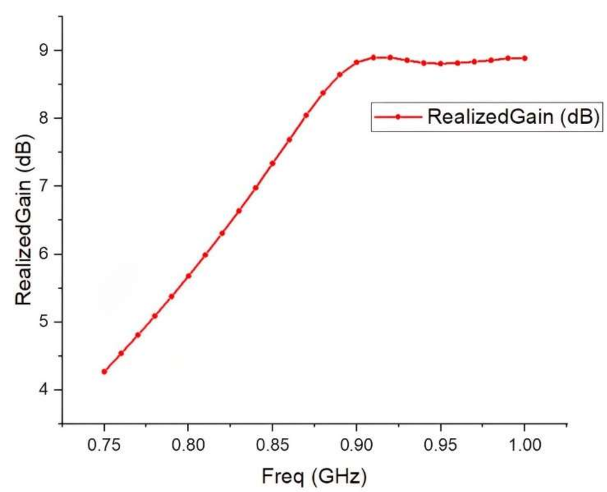

Figure 7. Simulated Realized Gain in the single element design.

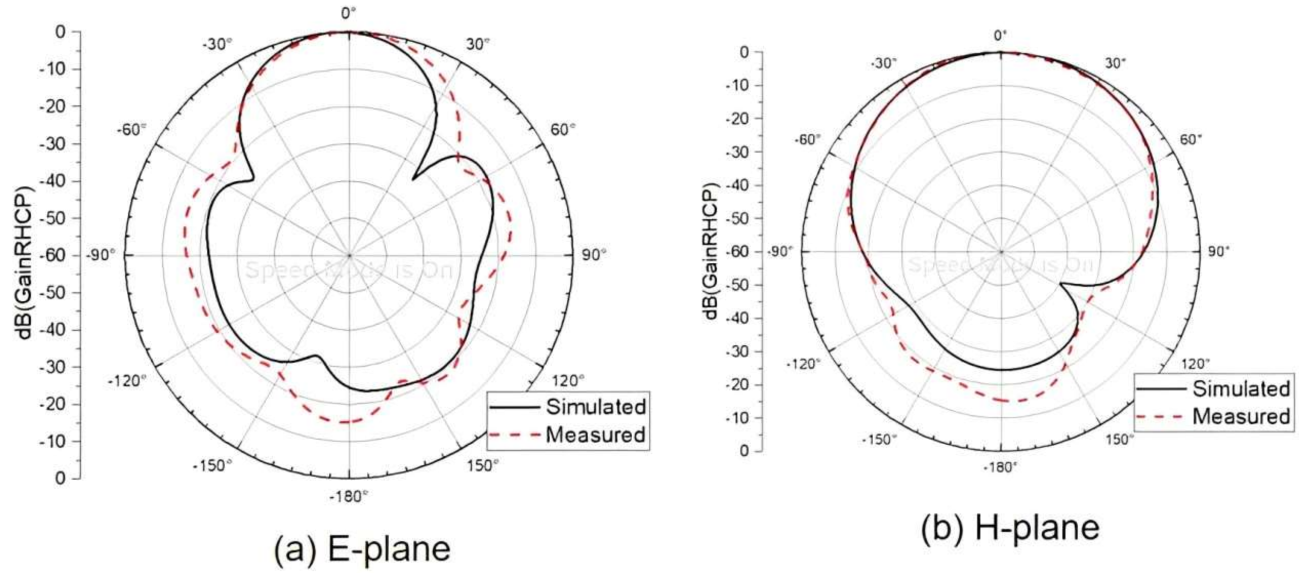

Figure 8. Radiation pattern at (a) phi=90, (b) phi=00 of the single element design.

4.2. Simulation results analysis of the array design

The research and design of a "metal-only micro-strip patch antenna and its array" have yielded compelling simulation results, showcasing the antenna's performance across various key metrics. This section provides a detailed exploration of the findings, focusing on a realized gain of 10.88 dB, a total gain of 11.2 dBi, an |S11| value of -20.8 dB, and an AR of less than 3 dB at 920 MHz. Additionally, the radiation pattern analysis, depicted in Figure 9, reveals the antenna's right-hand circular polarization, offering valuable insights into its directional characteristics.

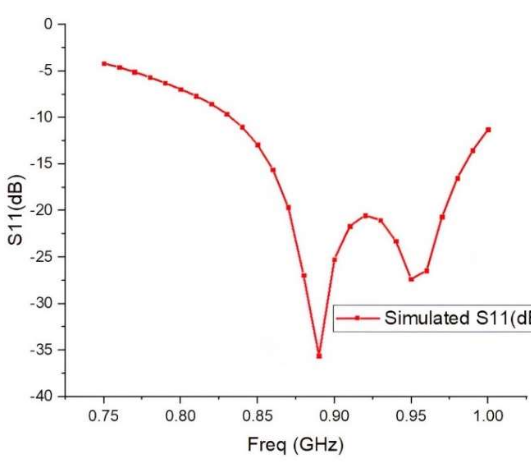

Figure 9. Simulated |S11| result of the array design.

The |S11| parameter, reflecting the return loss or reflection coefficient, plays a crucial role in evaluating the antenna's impedance matching. The obtained value of -20.8 dB at 920 MHz for |S11| is noteworthy, suggesting excellent impedance-matching characteristics. A lower return loss indicates minimal signal reflection, signifying efficient energy transfer from the transmitter to the antenna. This result bodes well for the antenna's overall performance, particularly in terms of maximizing power transfer and minimizing signal loss. The realized gain of 10.88 dB is a pivotal metric, representing the actual gain of the antenna while accounting for losses in the system, shown in Figure 10. This impressive figure underscores the efficiency of the antenna in converting input power into radiated energy.

Complementing this, the total gain of 11.2 dBi provides a comprehensive view of the antenna's ability to focus and direct the radiated signal, shown in Figure 11. A lower AR indicates superior CP quality, making the antenna well-suited for applications where polarization purity is crucial. This result is particularly important for communication systems and satellite links that rely on CP to maintain signal integrity during propagation.

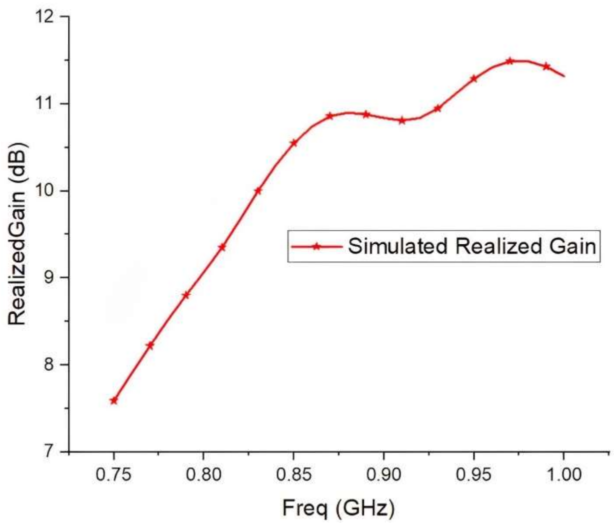

Figure 10. Simulated Realized Gain.

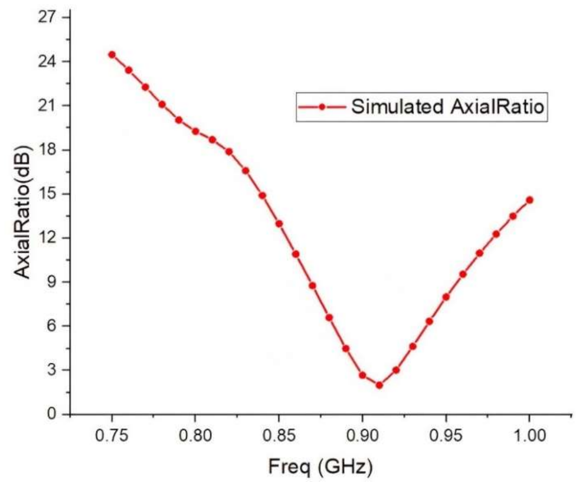

Figure 12. Simulated AR of the single element design.

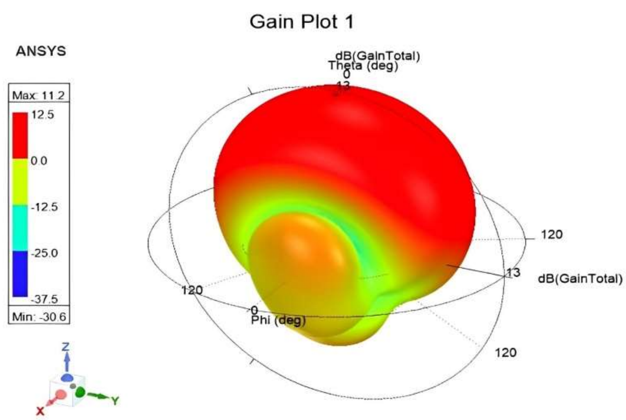

Figure 11. Simulated total gain of the single element design.

The AR is a critical parameter for circularly polarized antennas and achieving a value of less than 3 dB at 920 MHz is a significant accomplishment, in Figure 12.

Figure 13 presents the simulated radiation patterns at phi = 0 and phi = 90, respectively. These patterns offer valuable insights into the antenna's directional characteristics and polarization properties.

By observing the radiation pattern at phi = 00, the antenna exhibits a right-hand circular polarization. This polarization characteristic is confirmed by the analysis of the 3dB beam-width, which is approximately 720. The wide coverage area in the horizontal plane at phi = 00 suggests the antenna's suitability for applications requiring broad azimuthal coverage. At phi = 900, the radiation pattern narrows, and the 3dB beam-width reduces to around 360. This directional characteristic in the vertical plane signifies the antenna's ability to focus its radiation in a specific direction.

Finally, the simulated results of the "metal-only micro-strip patch antenna and its array" showcase a well-designed and high-performance antenna system. The realized gain, total gain, |S11| value, and AR metrics collectively indicate efficient energy transfer, excellent impedance matching, and superior CP at 920 MHz. The radiation pattern analysis further highlights the antenna's directional characteristics and its ability to provide broad coverage in the horizontal plane while focusing its radiation in the vertical plane.

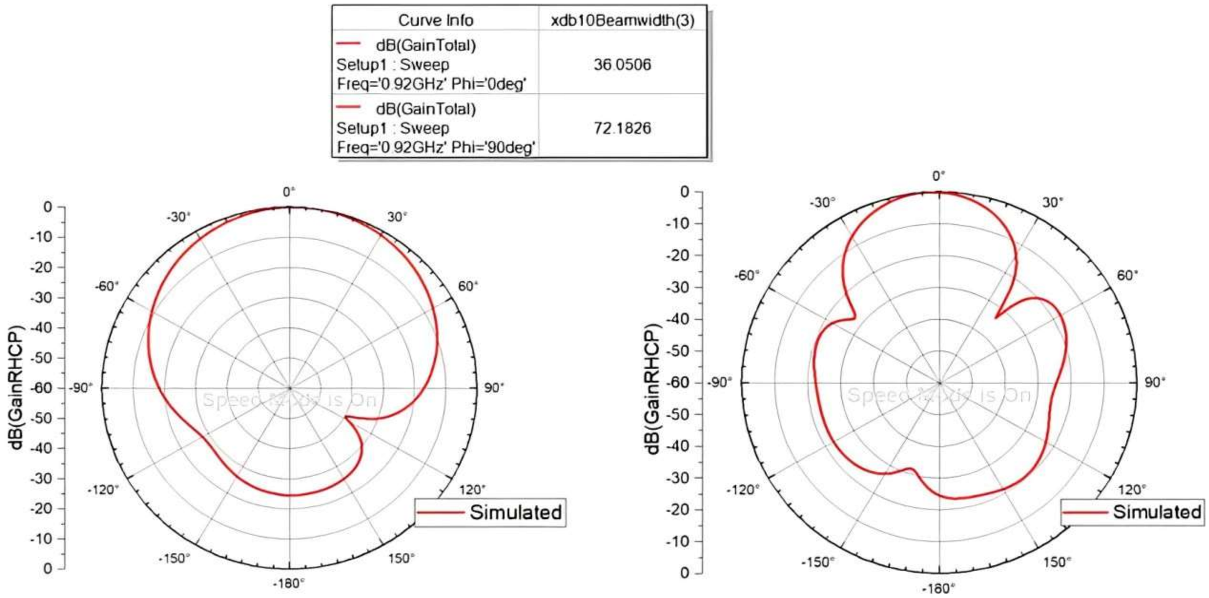

(a) Freequency-920MHz, Phi-90^0

(b) Freequency-920MHz, Phi-0^0

Figure 13. Radiation pattern at (a)phi=90^0 (b) phi=0^0 of the single element design.

4.3. Simulation results comparison analysis

4.3.1. Comparison

In terms of impedance matching, the |S11| parameter is a crucial indicator. The single-element design demonstrates a return loss of -18.94 dB at 920 MHz, while the array design exhibits a more favorable -20.8 dB. This suggests that the array design achieves superior impedance matching, resulting in reduced signal reflection and improved overall efficiency at the specified frequency.

4.3.2. Axial ratio

Both the single-element and array designs showcase an AR of less than 3 dB, emphasizing their excellence in circular polarization. This characteristic is particularly important in applications where maintaining polarization purity is critical for effective communication and signal reception. In Table 1., the total gain and realized gain metrics provide insights into the antenna's ability to focus and direct the radiated signal. The single-element design achieves a total gain of 9.1 dBi and a realized gain of 8.94 dB, while the array design surpasses these values with a total gain of 11.2 dBi and a realized gain of 10.88 dB.

Table 1. A comparison between the array design and single element simulation results.

Parameter	Single element design	Array design
|S11| (dB) at 920 MHz	-18.94	-20.8
AR (dB)	1.6	1.9
Total Gain (dBi)	9.1	11.2
Realized Gain (dB) at 920 MHz	8.94	10.88
3dB Beam-width (Degree), When phi=00	64	36
3dB Beam-width (Degree), When phi=900	67	72

These results suggest that the array design outperforms the single-element design in terms of overall gain, showcasing its potential for increased signal strength and coverage. In the single-element design, right-hand CP is evident, with a 3dB beam width of approximately 640 at phi = 00 and 670 at phi = 900. The array design also exhibits right-hand CP but, with notable differences in the 3dB beam width. At phi = 00, the beam width is around 720, offering a broader coverage area compared to the single-element design. However, at phi = 900, the array design's beam width narrows to 360, indicating a more directional focus compared to the single-element design.

4.4. Antenna processing and test analysis

In the pursuit of validating the accuracy and practical viability of the antenna model, a comprehensive process of simulation, optimization, and practical testing was executed. The intricacies multi-functional antenna is elucidated in Figure 14, depicting the tangible representation of the antenna's configuration and design.

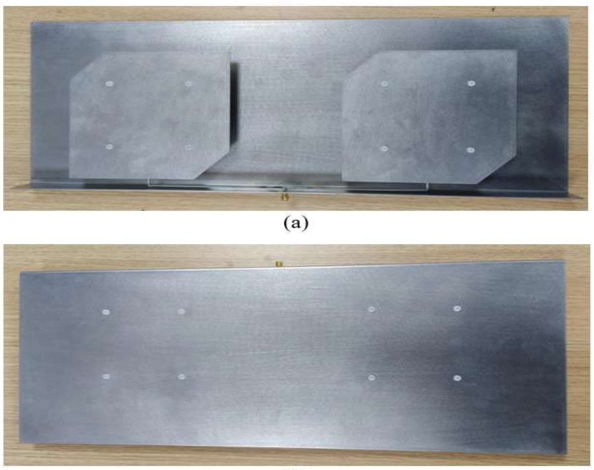

Figure 14. Antenna processing model: (a) Front side of the model; (b) Back side of the model.

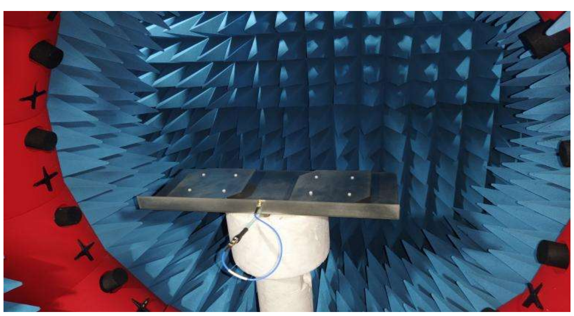

Figure 15. Prototype antenna under test in Anechoic Chamber.

The antenna stands, measuring 468 x 188 x 31 mm3, is a compact yet intricate design with a dielectric substrate of air and a copper radiation component. The ground plane is made of aluminum, aiming to optimize the antenna's performance. A 50-ohm coaxial feed is used for efficient signal transmission [25]. The Agilent E8361C model is used to assess the antenna's S parameters, a critical aspect of understanding its electrical characteristics. This advanced equipment allows for accurate measurements and evaluations of the antenna's performance, including gain response and radiation pattern, which are crucial metrics for determining its effectiveness in practical scenarios. In Figure 15, the antenna is securely affixed to a turntable for a systematic examination of its gain response and radiation pattern.

The antenna is tested using a Vector Network Analyzer (VNA), calibrated using E-Cal kits, and connected to the antenna port for precise measurements. Adherence to the coordinate axis direction is crucial for assessing antenna pattern and gain. The antenna is fixed on a turntable, and the directional pattern is elucidated by scanning it in various directions and measuring the received signal strength. The antenna's measured working center frequency is 920 MHz, with a simulated |S11| of -20.8, compared to an actual measurement of -18.21 dB, shown in Figure 16. This discrepancy may be due to factors like manufacturing tolerances, material properties, and environmental conditions [26]. The simulated bandwidth spans 833 MHz to 1 GHz, while the measured impedance bandwidth is around 840 MHz to 1 GHz. These differences highlight the need for practical validation to understand the antenna's behavior in real-world conditions and refine the model.

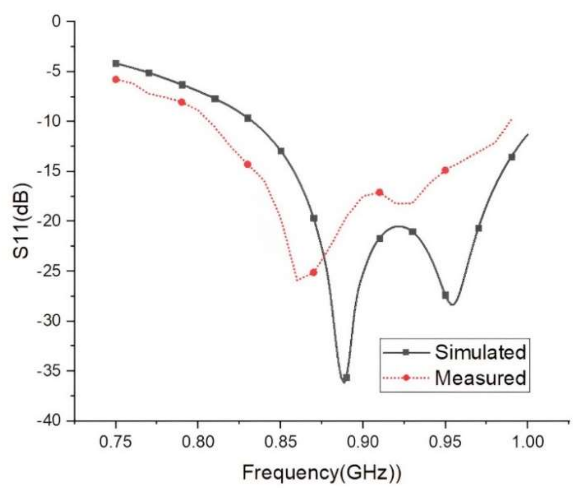

Figure 16. Comparing simulated and measured $|S_{11}|$.

The simulated results of a circularly polarized micro-strip patch antenna demonstrated consistent performance, with a 3dB beam width of 360 for the E-plane and 720 for the H-plane. The AR of the antenna was 2 dB, while the measured AR slightly deviates at 2.9 dB. The AR bandwidth spans 900 MHz to 920 MHz, with minor discrepancies due to fabrication tolerances, material variations, or measurement uncertainties.

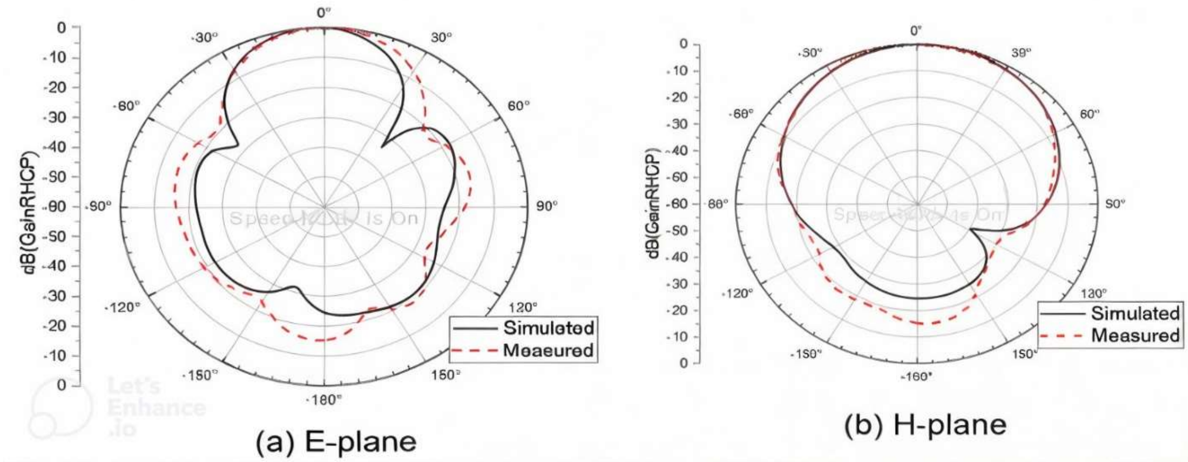

Figure 17. Normalized radiation pattern of antenna at 920 MHz: (a) E-Plane; (b) H-Plane.

The antenna's robustness and theoretical predictions' accuracy confirm its suitability for real-world applications [27]. Minor discrepancies may be due to fabrication tolerances, material variations, or measurement uncertainties. Overall, the antenna demonstrates promising CP performance. The performance of an antenna can be influenced by various factors, including the dielectric substrate material properties, processing accuracy during fabrication, precision in welding coaxial feed joints, potential errors in the testing environment, and human operations. The simulated realized gain at 920 MHz is 10.88 dBi, while the measured gain is slightly lower at 9.67 dBi, shown in Figure 17. These factors contribute to deviations between the simulated and measured results, shown in Table 2, emphasizing the importance of considering real-world conditions and imperfections in antenna performance evaluation, shown in Figure 18 and 19.

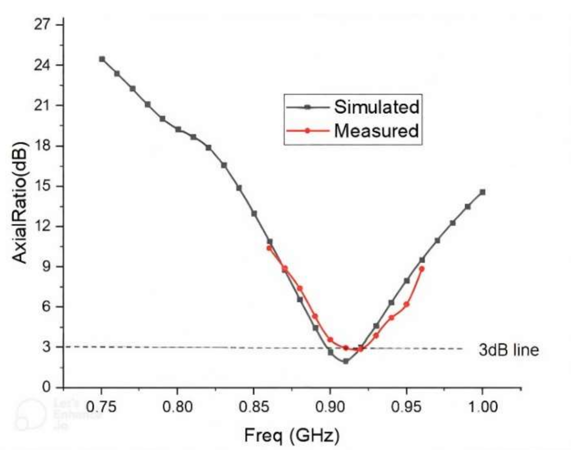

Figure 18. Comparison of simulated and measured axial ratio.

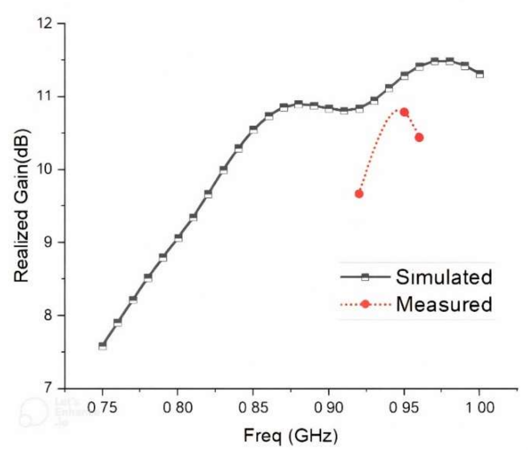

Figure 19. Simulated and measured realized gain.

Table 2. Comparing the measured and simulated values of the completing design

Parameter	Simulated	Measured
|S11| (dB) at 920MHz	-20.8	-18.21
AR(db)	2	2.9
AR bandwidth	900-920 MHz	910-920 MHz
Total Gain (dBi)	11.2	≤10.6
Realized Gain(dB) at 920 MHz	10.88	9.67

5. Discussion

The RFID system, also known as Extremely High Frequency (UHF), is a crucial wireless communication technology used in transportation and marketing. It involves an identifier, transmitter, and an RFID device, which generates microwave radiation using antennas. This electrical signal is then sent through the receiver, allowing data collection and analysis. RFID signals are particularly valuable in transportation and supplies; as transportable cellphones can capture data across vast distances. The simulated results of a circularly polarized micro-strip patch antenna demonstrated consistent performance, with a 3dB beam width of 360 for the E-plane and 720 for the H-plane. The performance of an antenna can be influenced by factors such as dielectric substrate material properties, processing accuracy during fabrication, precision in welding coaxial feed joints, potential errors in the testing environment, and human operations.

5.1. Increase operating effectiveness using UHF RFID technology

The growth of electronic commerce generated interest in accountability in consumable goods, prompting operational simplicity to enhance industrial as well as transportation workflows. RFID combined with UHF technological advances provides immediate information throughout a variety of commercial uses, including retailing, enhancing logistic network tracking, and increasing productivity. RFID signals may be used on a variety of items, including expensive outfits and even bottle caps, for bettering the management of stock operations. UHF sensors improve national control info precision, resulting in less inventories. RFID scanners may interpret more than 100 labels every second, enabling speedier dispatch of orders. RFID signals may identify unique items amid many identical ones, allowing you to recreate an entire supply chain chronology from the ingredient's origin to customer consuming. The system enables concurrent scanning of hundreds of tags per second at considerable lengths, decreasing inventory staff time by as much as 50%.

5.2. Advantages and applications of UHF RFID antenna

RFID, or UHF radio frequency identification, is a digital identifier with numerous benefits, including high entry, resilience to severe conditions, safety, and large memories. In China, UHF RFID air interfacing methods are prevalent for international, national, industrial, and commercial purposes. The Ultra High-Efficiency RFID Compatibility Circular Polarized Microstrip Antenna Array is a groundbreaking device that will transform powerful processes. Its compatibility using RF identification technology enables easy connectivity using other gadgets, as well as its radial polarity improves signal acquisition along with propagation whatever the direction, leaving it indispensable during those operations.

UHF RFID antennas offer increased scanning assortment, parallel scanning of multiple descriptions, excellent precision, and modularity. UHF RFID antennae can pass through substrates like wood, plastic, and paper, making them ideal for identifying items behind bundles and vessels. UHF RFID operates at frequencies ranging from 860 MHz to 960 MHz, provides a detection distance of as much as ten meters, but is capable of scanning numerous tags around the same time. Worldwide availability of UHF RFID digital identification bands varies, including China's bandwidth ranges, the EU bandwidth, Japan's 952MHz-954MHz, Hong Kong, Thailand, and Singapore's 920MHz-925MHz. UHF RFID scanning is rapidly expanding across business sectors, such as shopping centers, automobile flights, makeup, transportation, drugs, and agriculture. Remote UHF RFID is a common monitoring method due to quicker detection rates, extended detection separation, rapid data transfer velocity, excellent dependability, and tolerance for extreme conditions.

5.3. Disadvantages of UHF RFID technology

RFID technology, specifically UHF RFID, has many benefits over QR codes, namely rapid checking, fewer input of information mistakes, enhanced monitoring, as well as superior control of stocks. The downsides include contamination with metallic and fluids. Fortunately, Metalcraft's Universal RFID Asset Tag overcomes this problem. RFID devices are costlier than barcode scanners, however, the brief savings from utilizing RFID might prove worthwhile throughout the future. Regardless of such drawbacks, inactive UHF RFID labels may decrease energy and enhance the administration of stocks, allowing businesses to concentrate on other elements of the business.

6. Conclusion

The research and design of a state-of-the-art metal-only microstrip patch antenna and its arrays, specifically targeting the development of a UHF RFID-compatible circularly polarized microstrip antenna array, is presented. The proposed design, featuring a truncated patch with an air substrate, emphasizes high gain and circular polarization, with impressive results such as a return loss of less than -18.21 dB and a gain exceeding 10.6 dBi. A simulation analysis explores the performance of both single-element and array designs, positioning the array design as an excellent choice for applications requiring increased signal strength and coverage. A comparative analysis highlights the advantages of the array, emphasizing superior impedance matching and radiation patterns. Practical validation, utilizing advanced equipment and physical testing, shows strong agreement between simulated and measured results, affirming the robustness of the antenna design for real-world conditions.

Conflict of Interests

The Authors do not have any conflict of interests. Please read the Transparent Statement.

Data Availability Statement

All of our data is secure on our end. Due to copyright concerns, we are unable to disclose our proprietary data to readers.

Authors Contributions

All Authors contributed equally.

Transparent Statement

OMAR FARUQ as both author and editorial board member of *Science, Engineering and Technology* journal, confirm that the article underwent an independent peer review process. Reviewers were selected by the editorial team, and I did not participate in their selection or have access to their identities. The review process adhered to the highest standards of scholarly integrity.

Funding Declaration

The Authors did not receive any funds for the research, simulations and publication.

References

[1] Banerjee, U., Karmakar, A., & Saha, A. (2020). A review on circularly polarized antennas, trends and advances. *International Journal of Microwave and Wireless Technologies*, *12*(9), 922–943. https://doi.org/10.1017/S1759078720000331

[2] Munoz-Ausecha, C., Ruiz-Rosero, J., & Ramirez-Gonzalez, G. (2021). RFID Applications and Security Review. *Computation*, *9*(6), 69. https://doi.org/10.3390/computation9060069

[3] Reyes, P. M. (2023). Radio Frequency Identification (RFID) and Supply Chain Management. In *The Palgrave Handbook of Supply Chain Management* (pp. 1–35). Springer International Publishing. https://doi.org/10.1007/978-3-030-89822-9_109-1

[4] Zhang, J., Tian, G., Marindra, A., Sunny, A., & Zhao, A. (2017). A Review of Passive RFID Tag Antenna-Based Sensors and Systems for Structural Health Monitoring Applications. *Sensors*, *17*(2), 265. https://doi.org/10.3390/s17020265

[5] Rigall, E., Wang, X., Zhang, S., & Dong, J. (2023). A fast and accurate RFID tag positioning method based on AoA hologram and hashtables. *Computer Communications*, *202*, 135–144. https://doi.org/10.1016/j.comcom.2023.01.020

[6] Dey, S., & Karmakar, N. C. (2020). Design of novel super wide band antenna close to the fundamental dimension limit theory. *Scientific Reports*, *10*(1), 16306. https://doi.org/10.1038/s41598-020-73478-2

[7] Arun, H., & Alsath, M. G. N. (2019). Octagonal DGS based dual polarised ring-shaped antenna for MIMO communications. *International Journal of Electronics*, *106*(5), 756–769. https://doi.org/10.1080/00207217.2019.1570556

[8] Verma, A., Arrawatia, M., & Kumar, G. (2020). Broadband Series-fed Circularly Polarized Microstrip Antenna Array. *2020 IEEE International Symposium on Antennas and Propagation and North American Radio Science Meeting*, 225–226. https://doi.org/10.1109/IEEECONF35879.2020.9329489

[9] Garg, S., & Gowri, R. (2015). Circularly Polarized Antenna Array for L-Band Applications. *2015 IEEE International Conference on Computational Intelligence & Communication Technology*, 312–316. https://doi.org/10.1109/CICT.2015.121

[10] Prakasam, V., & Reddy, N. (2020). Design and Simulation of Elliptical Micro Strip Patch Antenna with Coaxial Probe Feeding for Satellites Applications Using Matlab. *2020 Fourth International Conference on I-SMAC (IoT in Social, Mobile, Analytics and Cloud) (I-*

SMAC), 228–234. https://doi.org/10.1109/I-SMAC49090.2020.9243472

[11] Akdag, I., Gocen, C., Palandoken, M., & Kaya, A. (2022). A novel circularly polarized reader antenna design for UHF RFID applications. *Wireless Networks*, *28*(6), 2625–2636. https://doi.org/10.1007/s11276-022-02998-8

[12] Karia, D. C., Dhengale, B. B., & Goswami, S. A. (2015b). A 1×2 array circularly polarised Microstrip antenna with a high Gain for RFID applications. *2015 International Conference on Computing and Network Communications (CoCoNet)*, 485–490. https://doi.org/10.1109/CoCoNet.2015.7411230

[13] Faudzi, N. M., Ibrahim, A., Mozi, A. M., & Hanaffi, W. N. A. (2021). Wideband slotted microstrip patch antenna for UHF-RFID reader. *Journal of Physics: Conference Series*, *1755*(1), 012028. https://doi.org/10.1088/1742-6596/1755/1/012028

[14] Das, T. K., Dwivedy, B., Behera, D., Behera, S. K., & Karmakar, N. C. (2020). Design and modelling of a compact circularly polarized antenna for RFID applications. *AEU - International Journal of Electronics and Communications*, *123*, 153313. https://doi.org/10.1016/j.aeue.2020.153313

[15] Nawaz, H., Niazi, A. U., & Ahmad, M. (2021). Dual Circularly Polarized Patch Antenna with Improved Interport Isolation for S-Band Satellite Communication. *International Journal of Antennas and Propagation*, *2021*, 1–10. https://doi.org/10.1155/2021/8022207

[16] Norzeli, S. M., Ismail, I., & Busu, M. F. M. (2012). Designing an UHF RFID reader antenna. *2012 IEEE Symposium on Humanities, Science and Engineering Research*, 599–602. https://doi.org/10.1109/SHUSER.2012.6268894

[17] Kashyap, N., G., Singh, D., & Sharma, N. (2022). Comprehensive Study of Microstrip Patch Antenna Using Different Feeding Techniques. *ECS Transactions*, *107*(1), 9545–9557. https://doi.org/10.1149/10701.9545ecst

[18] Krishna, A. M., R, V., Srivastavas, S., & Ranjan, N. (2023). Design of Ultra High Frequency (UHF) based RFID Reader for Electronic Toll-gate application. *2023 International Conference for Advancement in Technology (ICONAT)*, 1–5. https://doi.org/10.1109/ICONAT57137.2023.10080393

[19] Kawdungta, S., Mhunkaew, T., Torrungrueng, D., & Chou, H.-T. (2024). A Novel Antenna Design of Compact HF and UHF Passive RFID Tags with Interconnected Structure for Energy Harvesting and Tracking Systems. *International Journal of RF and Microwave Computer-Aided Engineering*, *2024*, 1–13. https://doi.org/10.1155/2024/9923732

[20] Erman, F., Hanafi, E., Lim, E.-H., Wan Mohd Mahyiddin, W. A., Harun, S. W., Umair, H., Soboh, R., & Makmud, M. Z. H. (2019). Miniature Compact Folded Dipole for Metal Mountable UHF RFID Tag Antenna. *Electronics*, *8*(6), 713. https://doi.org/10.3390/electronics8060713

[21] Tran-Huy, H., Nguyen, H.-H., & Hoang Thi Phuong, T. (2023). A compact metasurface-based circularly polarized antenna with high gain and high front-to-back ratio for RFID readers. *PLOS ONE*, *18*(8), e0288334. https://doi.org/10.1371/journal.pone.0288334

[22] Karia, D. C., Dhengale, B. B., & Goswami, S. A. (2015a). A 1×2 array circularly polarised Microstrip antenna with a high Gain for RFID applications. *2015 International Conference on Computing and Network Communications (CoCoNet)*, 485–490. https://doi.org/10.1109/CoCoNet.2015.7411230

[23] Z. Peterson, “The mysterious 50 Ohm impedance: Where it came from and why we use it,” Altium, 04-Mar-2021. [Online]. Available: https://resources.altium.com/p/mysterious-50-ohm-impedance-where-it-came-and-why-we-use-it. [Accessed: 18-May-2024].

[24] Zou, Z., Chen, Q., Uysal, I., & Zheng, L. (2014). Radio frequency identification enabled wireless sensing for intelligent food logistics. *Philosophical Transactions of the Royal Society A: Mathematical, Physical and Engineering Sciences*, *372*(2017), 20130313. https://doi.org/10.1098/rsta.2013.0313

[25] Kiriş, S., Alkurt, F. Ö., & Karaaslan, M. (2023). Pattern Shaping by Utilizing EBG Phase Response and Its Use in MIMO Radio Altimeter Antenna Design for Aircraft. *Electronics*, *12*(16), 3434. https://doi.org/10.3390/electronics12163434

[26] Kundu, K., Bhattacharya, A., Mohammed, F. H., & Pathak, N. N. (2023). Design and Analysis of a Low-profile Microstrip Antenna for 5G Applications using AI-based PSO Approach. *Journal of Telecommunications and Information Technology*, *3*(2023), 68–73. https://doi.org/10.26636/jtit.2023.3.1368

[27] Dastranj, A., Ranjbar, F., & Bornapour, M. (2019). A New Compact Circular Shape Fractal Antenna for Broadband Wireless Communication Applications. *Progress in Electromagnetics Research C*, *93*, 19–28. https://doi.org/10.2528/PIERC19031001